THE JOURNAL OF BIOLOGICAL CHEMISTRY VOL. 288, NO. 12, pp. 8222–8230, March 22, 2013

MicroRNA-140 Promotes Adipocyte Lineage Commitment of C3H10T1/2 Pluripotent Stem Cells via Targeting Osteopetrosis-associated Transmembrane Protein 1*[S]

Received for publication, October 10, 2012, and in revised form, January 31, 2013 Published, JBC Papers in Press, February 6, 2013, DOI 10.1074/jbc.M112.426163

Yuan Liu[‡§], Zhi-chun Zhang[‡], Shu-wen Qian[‡§], You-you Zhang[§], Hai-yan Huang[‡§], Yan Tang[‡], Liang Guo[‡], Xi Li[‡§1], and Qi-Qun Tang[‡§2]

From the [‡]Key Laboratory of Molecular Medicine, Ministry of Education, and the Department of Biochemistry and Molecular Biology, Fudan University Shanghai Medical College, Shanghai 200032 and the [§]Institute of Stem Cell Research and Regenerative Medicine, Institutes of Biomedical Sciences, Fudan University, Shanghai 200032, China

Background: BMP4 treatment induces adipocyte lineage commitment of C3H10T1/2 pluripotent stem cells.
Results: Expression of miR-140 increases significantly during adipocyte lineage commitment.
Conclusion: miR-140 promotes adipocyte lineage commitment through down-regulating *Ostm1*.
Significance: Which miRNA and how it functions in adipocyte lineage commitment are clarified.

BMP4 has been shown to induce C3H10T1/2 pluripotent stem cells to commit to adipocyte lineage. In addition to several proteins identified, microRNAs also play a critical role in the process. In this study, we identified microRNA-140 (miR-140) as a direct downstream component of the BMP4 signaling pathway during the commitment of C3H10T1/2 cells to adipocyte lineage. Overexpression of miR-140 in C3H10T1/2 cells promoted commitment, whereas knockdown of its expression led to impairment. Additional studies indicated that *Ostm1* is a *bona fide* target of miR-140, which is significantly decreased during commitment, and *Ostm1* was also demonstrated to function as an anti-adipogenic factor.

Obesity has become an escalating global epidemic since people have changed their diet and lifestyle in the 20th century; it not only affects appearance but also presents an array of serious disorders to health, including insulin resistance, type 2 diabetes, hypertension, and atherosclerosis (1, 2). Elucidating the mechanisms underlying obesity is critical for understanding obesity occurrence and progression. It has been shown that adipocyte development includes two progressive stages: lineage-restricted preadipocytes committed from pluripotent mesenchymal stem cells (3) and lipid-laden adipocytes differentiated from growth-arrested preadipocytes (4). Researchers have applied 3T3-L1 cells, a widely used preadipocyte cell line, to clearly understand the differentiation process (5, 6). However, there is still far more to learn about the commitment process (7).

The generally accepted mesenchymal stem cell line C3H10T1/2 has been used to elucidate the mechanisms of adipocyte lineage commitment (4). C3H10T1/2 cells are multipotent stem cells that can differentiate into various lineages, including osteocytes, chondrocytes, myocytes, and adipocytes (8, 9). BMP4 (bone morphogenetic protein 4) treatment can efficiently induce C3H10T1/2 cells to commit to adipocyte lineage through two downstream signaling pathways, SMAD and p38 MAPK (10). The commitment of C3H10T1/2 cells is accompanied by dramatic changes in cell shape, and several cytoskeleton-associated proteins (*i.e.* lysyl oxidase, TPT1 (tumor protein, translationally controlled 1), and αB-crystallin) have been demonstrated to be up-regulated by BMP4 during commitment (11).

MicroRNAs (miRNAs)[3] function at the post-transcriptional level by negatively regulating mRNA stability or translation, and they participate in almost every physiological and pathological process (12–15). Numerous miRNAs have been shown to be involved in terminal adipocyte differentiation (16). For example, microRNA (miR)-143, a well known miRNA that enhances adipogenesis, increases after induction of differentiation and targets pleiotrophin to promote differentiation of 3T3-L1 preadipocytes (17), whereas pleiotrophin plays a negative role during adipogenesis through the pleiotrophin/PI3K/Akt/GSK3β/β-catenin signaling pathway. Stable transfection of 3T3-L1 cells with the miR-17-92 cluster results in accelerated differentiation by negatively regulating the tumor suppressor protein Rb2/p130, which participates in a fundamental step in mitotic clonal expansion (18). miR-375 enhances 3T3-L1

* This work supported in part by National Key Basic Research Project Grants 2011CB910201 and 2011CBA01103, State Key Program of National Natural Science Foundation Grant 31030048, and Shanghai Key Science and Technology Research Project Grant 10JC1401000 (to Q.-q. T.); National Natural Science Foundation Grants 81270954 and 30870510 and Shanghai Rising Star Program Grant 08QA14012 (to X. L.); and Shanghai Leading Academic Discipline Project Grants B110 and 985III-YFX0302 (to the Department of Biochemistry and Molecular Biology, Fudan University Shanghai Medical College).
[S] This article contains supplemental "Experimental Procedures" and Figs. S1–S3.
[1] To whom correspondence may be addressed: Key Laboratory of Molecular Medicine, Ministry of Education, and Department of Biochemistry and Molecular Biology, Fudan University Shanghai Medical College, Shanghai 200032, China. E-mail: lixi@shmu.edu.cn.
[2] To whom correspondence may be addressed: Key Laboratory of Molecular Medicine, Ministry of Education, and Department of Biochemistry and Molecular Biology, Fudan University Shanghai Medical College, Shanghai 200032, China. Tel.: 86-21-5423-7198; Fax: 86-21-5423-7290; E-mail: qqtang@shmu.edu.cn.

[3] The abbreviations used are: miRNA/miR, microRNA; MSCV, murine stem cell virus; qRT-PCR, quantitative RT-PCR.

adipocyte differentiation by suppressing the phosphorylation levels of ERK1/2 (19). On the other hand, the miR-27 gene family, including miR-27a and miR-27b, is down-regulated during 3T3-L1 adipocyte differentiation, and overexpression of miR-27a and miR-27b inhibits adipocyte differentiation of 3T3-L1 preadipocytes (20). The miR-27 family has also been shown to be elevated in obese mice and to contribute to LPS-mediated inflammation by targeting peroxisome proliferator-activated receptor γ (21). However, there is little information regarding the roles of miRNAs during adipocyte lineage commitment.

OSTM1 is a type I transmembrane protein that localizes in intracellular vesicles, is highly expressed in cartilage, and is generally conserved in a wide range of species, including zebrafish, mice, and humans (25, 26). Previous studies elucidated three biological functions of OSTM1: it serves as a β-subunit of ClC-7 to support bone resorption and lysosomal function, it works as an E3 ubiquitin ligase to induce proteasome-dependent degradation of $G\alpha_{i3}$, and it promotes β-catenin/Lef1 interaction (22–24). The above findings suggest that OSTM1 has an important role in bone development. As mesenchymal stem cells can differentiate into both osteocytes and adipocytes, OSTM1 might influence cell fate determination between these cells.

In this study, we found that BMP4 treatment dramatically increased miR-140 expression, which promoted the commitment of C3H10T1/2 cells to adipocyte lineage. Furthermore, we identified *Ostm1* as a direct target of miR-140 and show that it functions as an anti-adipogenic factor.

EXPERIMENTAL PROCEDURES

Cell Culture and Induction of Commitment and Differentiation—C3H10T1/2 mesenchymal stem cells and 3T3-L1 preadipocytes were propagated and differentiated as described (4).

Construction of Plasmids—The miR-140 expression plasmid MSCV-miR-140 was generated using standard DNA cloning techniques. The mouse miR-140 precursor, including ~670 bp of genomic flanking sequence, was cloned between the BglII (5′-end) and XhoI (3′-end) restriction sites of the MSCV vector using the following primer pair: forward, 5′-CCGAGATCTAGCATTGCCGTGGACAACAG-3′; and reverse, 5′-CCGCTCGAGCTTCAGGGTACCCCATAGGT-3′.

A 50-bp fragment of the *Ostm1* 3′-UTR containing the predicted binding site for miR-140 was cloned between the XhoI (5′-end) and NotI (3′-end) restriction sites using primers 5′-TCGAGTACCTTTCAGTACTGTGTGTACAAACCACTGCTTTTGGCTAAGAAGCTGGGC-3′ (forward) and 5′-GGCCGCCCAGCTTCTTAGCCAAAAGCAGTGGTTTGTACACACAGTACTGAAAGGTAC-3′ (reverse). Each oligonucleotide contained a predicted miR-140-binding site (underlined). The sites mutated in the oligonucleotides were as follows: forward, 5′-TCGAGTACCTTTCAGTACTGTGTGTACATTGGTGAGCTTTTGGCTAAGAAGCTGGGC-3′; and reverse, 5′-GGCCGCCCAGCTTCTTAGCCAAAAGCTCACCAATGTACACACAGTACTGAAAGGTAC-3′. Both oligonucleotides were annealed and cloned into the psiCHECK2 vector downstream of the *Renilla* luciferase reporter gene.

The *Ostm1* gene coding DNA sequence was amplified using primers 5′-CCGCTCGAGATGGCTCGGGACGCGGAGCT-3′ (forward) and 5′-GGAATTCTCAGGTGGCATTTTCTTGAAT-3′ (reverse) and cloned between the XhoI (5′-end) and EcoRI (3′-end) restriction sites of the MSCV vector (GenBank™ accession number NM_172416.3). The MiR-140 sponge was a generous gift from Dr. Xizhi Guo (Bio-X Center, Shanghai Jiao Tong University).

Microarray and Data Analysis—Total RNA was extracted using the TRIzol method (Invitrogen) according to the manufacturer's protocol. miRNA microarray was performed using Agilent mouse miRNA microarrays in triplicate.

Quantitative RT-PCR Analysis—Total RNA (including total miRNA) was harvested from C3H10T1/2 cells using TRIzol. The miRNA was reverse-transcribed using the TaqMan miRNA reverse transcription kit (Applied Biosystems) and miRNA-specific primers (Applied Biosystems). miRNA expression levels were then analyzed using the appropriate TaqMan miRNA assay (Applied Biosystems) according to the manufacturer's instructions. Quantitation of the ubiquitously expressed miRNA (U6) was performed as an endogenous control.

To determine the expression level of *Ostm1*, the mRNA was reverse-transcribed using the RevertAid™ first-strand cDNA synthesis kit (Fermentas) with random primers, followed by real-time PCR with SYBR Green chemistry (Applied Biosystems). Primer sequences were as follows: *Ostm1*, 5′-GAGCTGACCGCCTGTATGG-3′ (forward) and 5′-ATGTTTCGGCTGATGTTGTCC-3′ (reverse); and GAPDH, 5′-GGCAAATTCAACGGCACAGT-3′ (forward) and 5′-CGCTCCTGGAAGATGGTGAT-3′ (reverse).

Oil Red O Staining—Cells were washed three times with PBS and fixed for 15 min with 3.7% formaldehyde. Oil Red O (0.5% in isopropyl alcohol) was diluted with water (3:2), filtered through a 0.45-μm filter, and incubated with the fixed cells for 1 h at room temperature. Cells were then washed with water, and stained lipid droplets in the cells were visualized by light microscopy and photographed.

Luciferase Assay—293T cells were transfected with 10 ng of psiCHECK2-*Ostm1* 3′-UTR vector at 24 h after plating and with psiCHECK2-mutant *Ostm1* 3′-UTR vector and miR-140 sponge vector for 6 h in reduced serum and antibiotic-free Opti-MEM I with Lipofectamine 2000. Cells were cotransfected with the miR-140 mimic or a negative control (Genepharm) at 100 nM. Firefly and *Renilla* luciferases were measured in cell lysates using the Dual-Luciferase reporter assay system (Promega). Firefly luciferase activity was used for normalization and as an internal control for transfection efficiency.

Transfection Assay—Transfection experiments were performed with Lipofectamine™ 2000 and Lipofectamine™ RNAiMAX (Invitrogen) following the manufacturer's instruction.

RNA Interference—Synthetic siRNA oligonucleotides specific for *Smad4* (GenBank™ accession number NM_008540.2), p38 MAPK (GenBank™ accession U10871.1), and *Ostm1* mRNAs were designed and synthesized by Invitrogen Stealth™ RNAi. The sequences were as follows: *Smad4* Stealth™ RNAi, 5′-CAUACACACCUAAUUUGCCUCACCA-3′; p38 MAPK Stealth™ RNAi, 5′-CCUUUGAAAGCA-

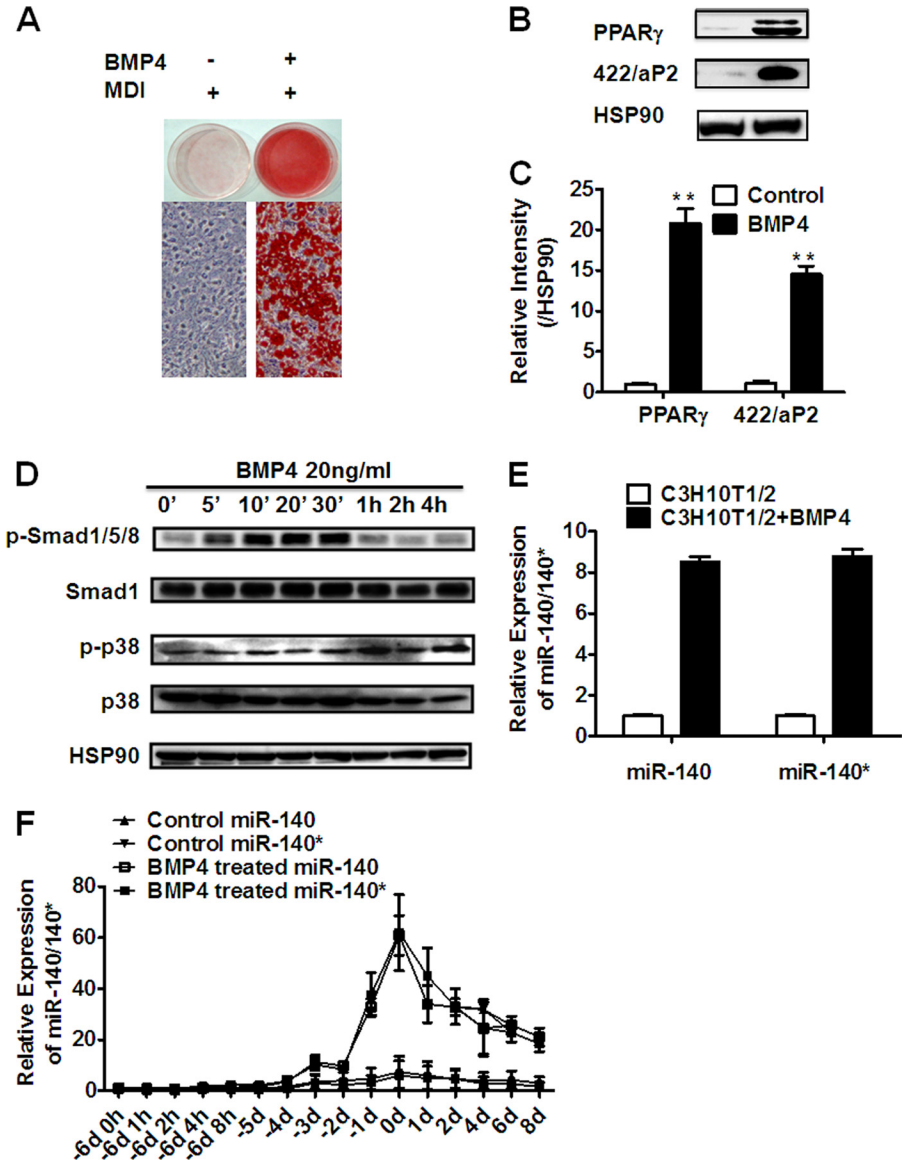

FIGURE 1. **miR-140 and miR-140* are induced during adipocyte lineage commitment of C3H10T1/2 cells after BMP4 treatment.** C3H10T1/2 stem cells plated at low density (day −6) were treated without or with BMP4 for 6 days until post-confluent and then subjected to the adipocyte differentiation protocol to day 7. *MDI,* adipogenic cocktail containing MIX, DEX and insulin; *MIX,* methylisobutylxanthine. *A* and *B*, on day 7, Oil Red O staining and Western blotting were performed to confirm adipogenesis. *PPARγ*, peroxisome proliferator-activated receptor γ. *C*, the relative intensity of the Western blots in *B* was determined in three independent experiments. *D*, activation of the BMP4 signal was demonstrated by phosphorylation of p38 MAPK and SMAD1/5/8 by Western blotting on day 0. *E*, miR-140 and miR-140* expression levels were detected on day 0 by quantitative RT-PCR (qRT-PCR). Each *bar* represents the mean ± S.D. of three independent experiments. *F*, miR-140 and miR-140* expression patterns during C3H10T1/2 cell adipogenesis were assessed by qRT-PCR (day (*d*) −6 to day 7). Each *point* represents the mean ± S.D. of three independent experiments. *C,* relative intensity of Western blotting in B was performed through three independent experiments. **, $p < 0.01$.

GGGACCUUCUCAU-3′; and *Ostm1* Stealth™ RNAi. 5′-GAGCUGCUGAUGGACUUCGCCAAUA-3′.

Isolation of Stromal Vascular Fraction—Epididymal and inguinal fat pads from male C57BL/6 mice and wild-type and BMP4 transgenic mice in which BMP4 was specifically overexpressed in adipose tissue were excised and minced in PBS with 0.5% BSA. Collagenase (Sigma-Aldrich) was added to 1 mg/ml before incubation at 37 °C for 2 h with shaking. Suspensions were centrifuged at 1500 × *g* for 5 min to remove cellular debris and oil; precipitations were resuspended with RBC lysis buffer and then recentrifuged at 4000 × *g* for 10 min. Suspensions were washed twice with PBS, centrifuged, and resuspended with cell lysis buffer. Samples were heated at 110 °C for 15 min and were then ready for Western blotting.

RESULTS

miR-140 and miR-140 Are Induced during Adipocyte Lineage Commitment of C3H10T1/2 Cells by BMP4 Treatment*—As shown in Fig. 1 (*A* and *B*), we confirmed that BMP4 can induce commitment of C3H10T1/2 cells from pluripotent stem cells to adipocyte lineage (4), and activation of BMP4 signaling, *e.g.* phosphorylation of p38 MAPK and SMAD1/5/8, was significantly induced (Fig. 1*D*). To determine whether miRNA is involved in this process, microarray analysis was performed,

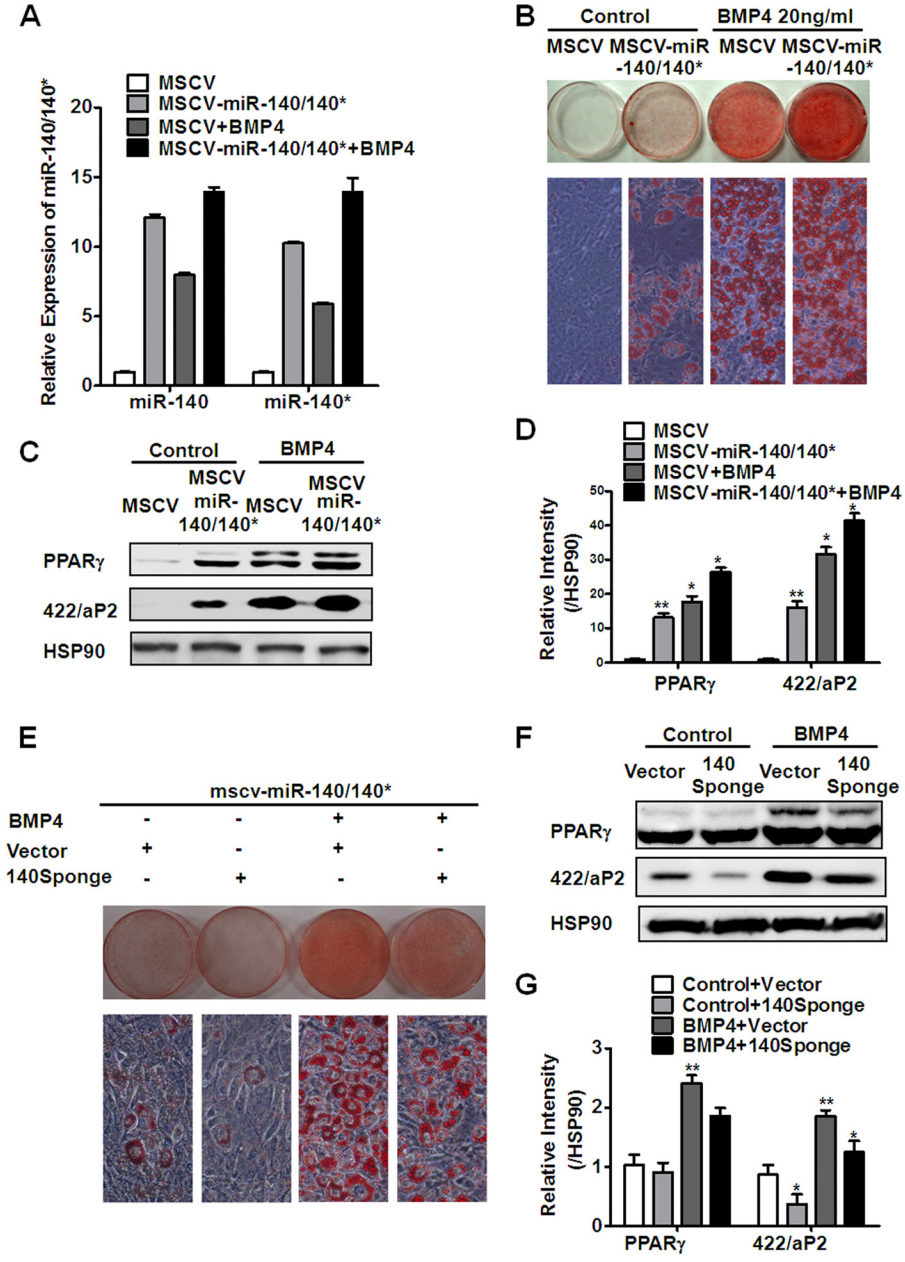

FIGURE 2. **miR-140 promotes adipocyte lineage commitment of C3H10T1/2 cells.** C3H10T1/2 stem cells were infected with MSCV or MSCV-miR-140/140*. *A*, 2 days post-confluence, total RNA was isolated and subjected to qRT-PCR to confirm the overexpression of miR-140 and miR-140*. Each *bar* represents the mean ± S.D. of three independent experiments. *B* and *C*, upon reaching post-confluence, cells were induced to differentiate with the standard adipocyte differentiation protocol, and on day 7, Oil Red O staining and Western blotting were performed to analyze the adipogenesis. *PPARγ*, peroxisome proliferator-activated receptor γ. *D*, the relative intensity of the Western blots in *C* was determined in three independent experiments. *E* and *F*, MSCV-miR-140/140*-infected C3H10T1/2 cells were transfected with empty pEGFP or pEGFP-miR-140 sponge vector and treated with BMP4 or not until post-confluent. Cells were subjected to the adipocyte differentiation protocol up to day 7. Oil Red O staining and Western blotting were performed to analyze adipogenesis. *G*, the relative intensity of the Western blots in *F* was determined in three independent experiments. *D*, relative intensity of western blotting in *C* was performed through three independent experiments. *, $p < 0.05$; **, $p < 0.01$.

and the results revealed that numerous miRNAs were positively or negatively regulated by BMP4 treatment (supplemental Fig. S1). In addition to many slightly altered miRNAs, miR-140 and miR-140* increased by >2-fold in BMP4-treated C3H10T1/2 cells compared with control cells and were selected for further studies. Because miR-140 and miR-140* originated from two strands of one single pre-miRNA, their expression levels were determined by TaqMan real-time PCR assay (Fig. 1*E*). As illustrated in Fig. 1*F*, the expression of miR-140 and miR-140* began to increase gradually during commitment, peaked on day 6 after continuous BMP4 treatment, and decreased during terminal adipocyte differentiation, which implied that they might function in adipocyte lineage commitment. In contrast, the miRNA expression level changed slightly in control C3H10T1/2 cells compared BMP4-treated cells.

miR-140 Overexpression Promotes Adipocyte Lineage Commitment of C3H10T1/2 Cells—Because miR-140 and miR-140* were specifically enriched during BMP4-induced C3H10T1/2 cell commitment, we hypothesized that their introduction into C3H10T1/2 cells might bias cells toward a preadipocyte line-

age. Because miR-140 and miR-140* come from the same precursor, their overexpression could not be separated. However, because miR-140* is usually degraded merely as a carrier strand, and miR-140 has been reported to function during mesoderm development, we focused our research mainly on miR-140. We constructed the miRNA-overexpressing plasmid MSCV-miR-140/140* by cloning the miR-140/140* precursor into the MSCV vector, followed by infection in C3H10T1/2 cells. Real-time PCR confirmed that the overexpression was effective (Fig. 2*A*). miR-140/140*-overexpressing C3H10T1/2 cells could partially differentiate into mature adipocytes even without BMP4 treatment. Furthermore, treatment with BMP4 before confluence significantly boosted their adipogenic capacity as indicated by Oil Red O staining of fat droplet accumulation and Western blot analysis of adipocyte-specific markers (Fig. 2, *B* and *C*). These results, combined with the miRNA expression pattern showed in Fig. 1*E*, indicate that miRNAs play a critical role during the adipocyte lineage commitment of C3H10T1/2 cells. Thereafter, the miR-140 sponge vector was used to decrease miR-140 expression in miRNA-overexpressing C3H10T1/2 cells after BMP4 treatment (27). The effect of the sponge is shown in Fig. 3*E*. Consistent with our assumption, the increase in adipogenesis upon miRNA overexpression was significantly decreased after the introduction of the miR-140 sponge (Fig. 2, *E* and *F*). This confirms that miR-140 plays a very important role during commitment.

Identification of OSTM1 as a Target Protein of miR-140 during Adipocyte Lineage Commitment of C3H10T1/2 Cells—PicTar, TargetScan, and Miranda were used to identify putative target proteins of miR-140 that overlapped among these three algorithms (28). We found that most of the genes in the list matched those from the Dual-Luciferase experiments (supplemental Fig. S2); however, only a few of them could be eventually demonstrated to be coordinately regulated during the same physiological process. Accordingly, *Ostm1* was markedly down-regulated at both the protein and mRNA levels when miR-140 was overexpressed in C3H10T1/2 cells (Fig. 3, *A* and *B*). Furthermore, the repressive function of BMP4 or miR-140 on the expression of *Ostm1* could be predominantly reversed by the miR-140 sponge, which could bind to miR-140 and diminish its repression of the target protein (Fig. 3*C*).

According to the sequence analysis, *Ostm1* contains two 7-nucleotide sites within its 3′-UTR, which matched the seed region of miR-140. These two putative miRNA-binding sites were cloned into the psiCHECK2 vector, respectively, and only one site bound miR-140 (Fig. 3*D*). Compared with the negative control miRNA mimic, cotransfection of the *Ostm1* 3′-UTR-luciferase reporter with the miR-140 mimic resulted in significantly repressed luciferase activity. Correspondingly, miR-140 had no effects on the mutant *Ostm1* 3′-UTR-reporters. Furthermore, when the miR-140 sponge vector was used to neutralize the effects of the miR-140 mimic, no difference in luciferase activity could be observed between control mimic- and miR-140 mimic-transfected cells (Fig. 3*E*). These results indicate that *Ostm1* is a direct target of miR-140.

Ostm1 Is Identified as an Anti-adipogenic Factor, and Its Expression Is Decreased by BMP4 through miR-140 during Adipocyte Lineage Commitment of C3H10T1/2 Cells—Western blotting was used to detect OSTM1 expression during the commitment stage in C3H10T1/2 cells. Compared with control C3H10T1/2 cells, OSTM1 expression was significantly decreased in BMP4-treated cells (Fig. 4*A*). In previous studies, SMAD and p38 MAPK were downstream of the BMP4 signaling pathway in the commitment of C3H10T1/2 stem cells to adipocyte lineage. Specific Stealth™ RNAi was used to define regulation of the BMP signaling pathway upon expression of miR-140 (10). miR-140 was observed to be significantly repressed by p38 MAPK and *Smad4* RNAi, respectively (Fig. 4*B*). In addition, p38 MAPK and *Smad4* RNAi successfully res-

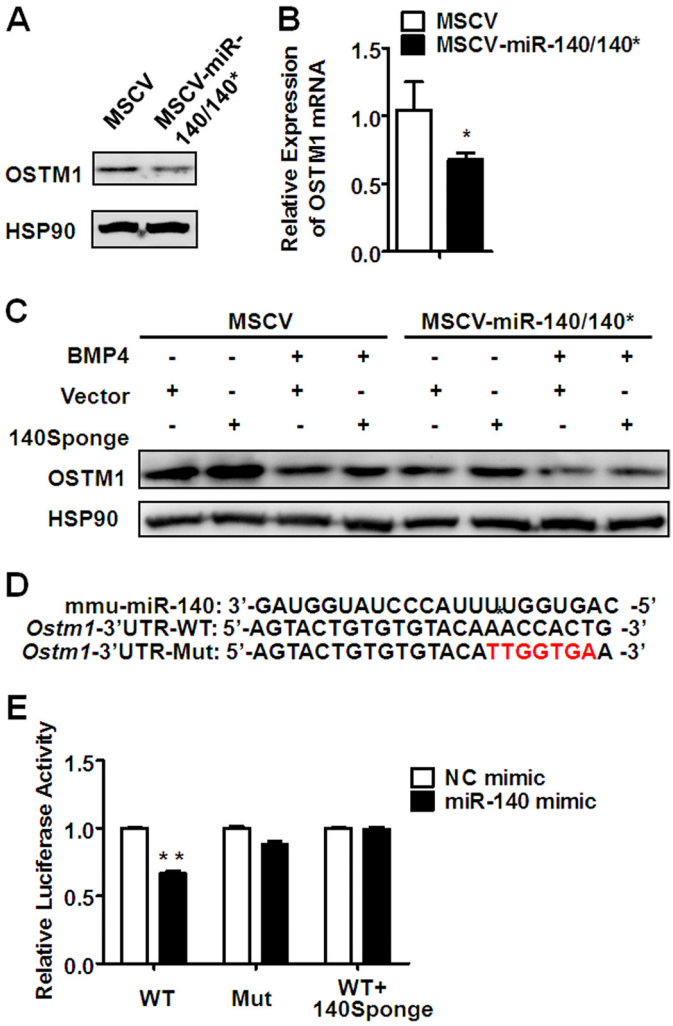

FIGURE 3. **Identification of OSTM1 as a target protein of miR-140 during C3H10T1/2 cell commitment.** *A* and *B*, Western blotting and qRT-PCR were performed to detect *Ostm1* expression during the commitment of C3H10T1/2 cells. Each *column* represents the mean ± S.D. of three independent experiments. *, $p < 0.05$. *C*, MSCV-miR-140/140*-infected C3H10T1/2 cells were transfected with empty pEGFP or pEGFP-miR-140 sponge vector and treated with BMP4 or not until post-confluent. Cells were then subjected to Western blotting to detect OSTM1 expression. *D*, schematic of the miR-140 putative target site in the *Ostm1* 3′-UTR. *mmu*, Mus musculus. *E*, 293T cells were transfected with 10 ng of empty psiCHECK2, psiCHECK2-*Ostm1*, or psiCHECK2-mutant *Ostm1* vector and 0.8 μg of empty pEGFP or pEGFP-miR-140 sponge vector. Cells were cotransfected with 100 nM miR-140 mimic or a negative control (*NC*). Firefly and *Renilla* luciferases were measured in cell lysates, and values were normalized to the psiCHECK2 vector and are presented as -fold change. Each *bar* represents the mean ± S.D. of three independent experiments. **, $p < 0.01$.

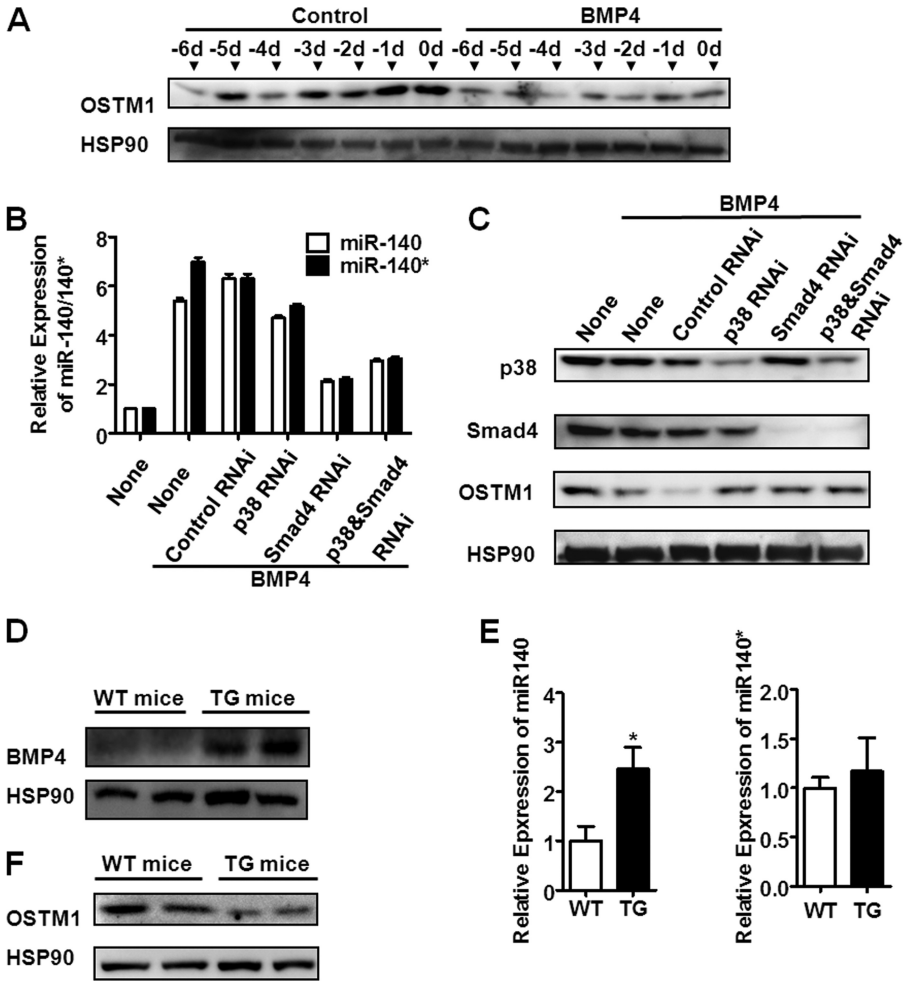

FIGURE 4. **BMP4 decreases *Ostm1* expression through miR-140.** *A*, cell lysates were collected each day during commitment and subjected to Western blotting. *d*, day. *B* and *C*, C3H10T1/2 stem cells were plated at 30% confluence and transfected with *Smad4* or p38 MAPK Stealth™ RNAi; and 24 h later, they were treated with BMP4 or not until post-confluent. Expression of miR-140 and miR-140* was determined by qRT-PCR, and expression of p38 MAPK, SMAD4, and OSTM1 was determined by Western blotting. Each *bar* represents the mean ± S.D. of three independent experiments. *D*, transgenic (*TG*) mice overexpress BMP4 in adipose tissue. Western blotting was performed to detect BMP4 expression levels in white adipose tissue (subcutaneous) from wild-type and aP2-BMP4 transgenic mice. *E* and *F*, the stromal vascular fraction was isolated from wild-type and transgenic mice to determine miRNA and protein levels. *, $p < 0.05$.

cued BMP4-induced *Ostm1* repression compared with control RNAi (Fig. 4*C*), and their relationship was further confirmed in aP2-BMP4 transgenic mice, in which BMP4 is overexpressed specifically in adipocytes (Fig. 4*D*). The stromal vascular fraction was isolated from the adipose tissue of wild-type and transgenic mice. *Ostm1* expression was dramatically decreased in BMP4-overexpressing mice in correlation with miR-140 upregulation in the stromal vascular fraction (Fig. 4, *E* and *F*). These results indicate that *Ostm1* is decreased by BMP4 through miR-140 during adipocyte lineage commitment.

On the basis of the above results, we assumed that OSTM1 might function as an anti-adipogenic factor. As shown in Fig. 5 (*C* and *D*), adipocyte differentiation was significantly impaired in *Ostm1*-overexpressing C3H10T1/2 cells as indicated by Oil Red O staining and Western blot analysis of adipocyte-specific markers. Moreover, when *Ostm1* expression was knocked down by siRNA (Fig. 5*F*), an apparent increase in adipogenic ability was observed. A half-dosage of BMP4 resulted in >70% adipogenesis when *Ostm1* was knocked down compared with <10% adipogenesis in the control (Fig. 5, *G* and *H*). To further confirm that targeting *Ostm1* is important for the pro-adipogenic function of miR-140, knockdown of *Ostm1* was performed in miR-140-overexpressing C3H10T1/2 cells. In the presence of BMP4 treatment, there was no significant difference between the control group and the *Ostm1* knockdown group (supplemental Fig. S3), possibly because BMP4 treatment of miR-140-overexpressing cells would lead to nearly total adipogenesis. However, in the absence of BMP4 treatment, knockdown of *Ostm1* enhanced the pro-adipogenic effect of miR-140 (supplemental Fig. S3), indicating that *Ostm1* is an important target of miR-140 during adipocyte lineage commitment. These results demonstrate that *Ostm1* functions as an anti-adipogenic factor and is an important target gene of miR-140 in BMP4-induced commitment of C3H10T1/2 stem cells.

DISCUSSION

Mesenchymal stem cells are multipotent stem cells that can differentiate into a variety of cell types, including osteocytes, chondrocytes, myocytes, and adipocytes (8, 29). Adipogenesis

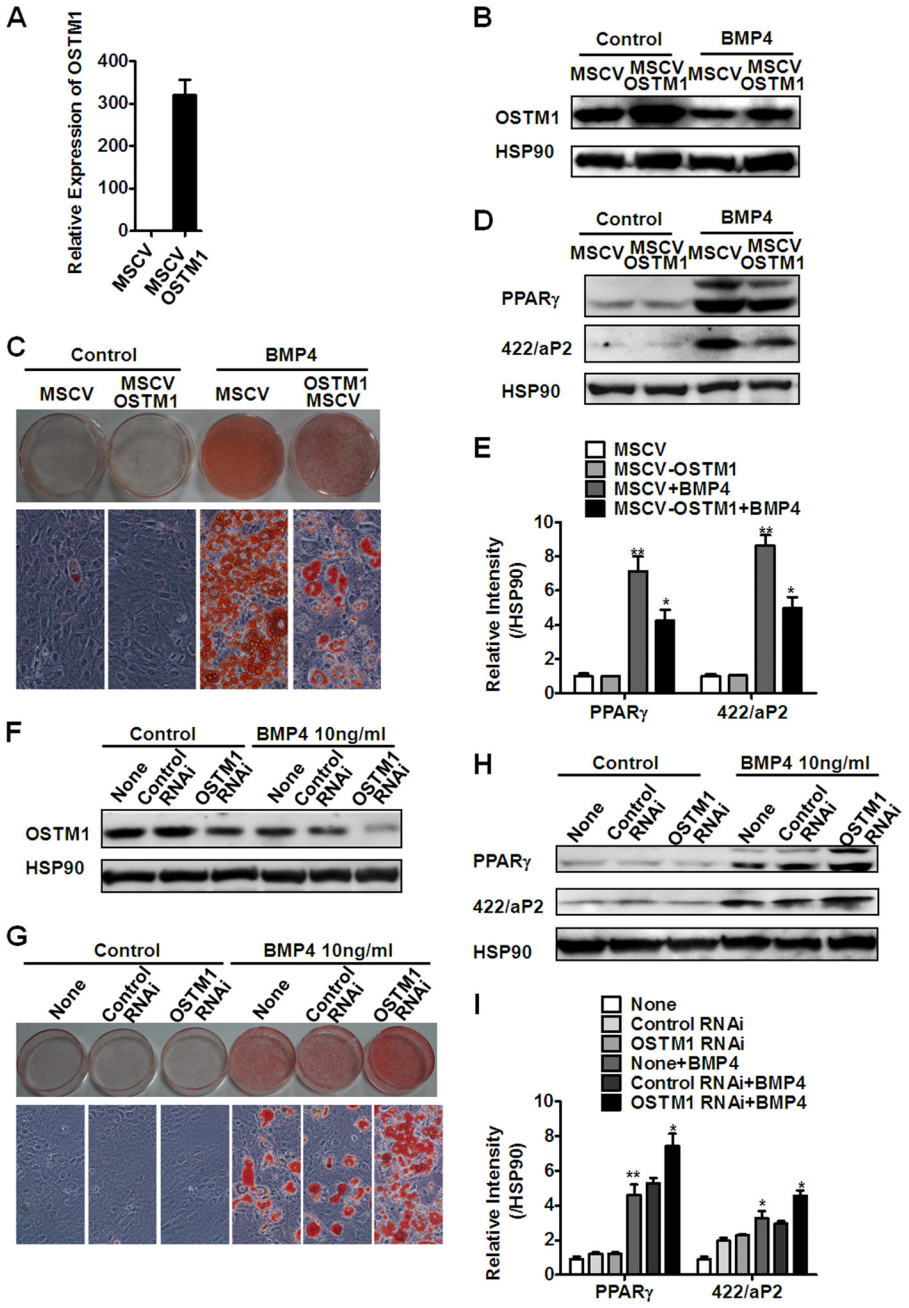

FIGURE 5. **OSTM1 functions as an anti-adipogenic factor during adipocyte lineage commitment of C3H10T1/2 cells.** *A* and *B*, C3H10T1/2 cells were infected with MSCV or MSCV-OSTM1. Two days post-confluence, qRT-PCR and Western blotting were performed to confirm the overexpression of *Ostm1*. Each *bar* represents the mean ± S.D. of three independent experiments. *C* and *D*, upon reaching post-confluence, cells were induced to differentiate with the standard adipocyte differentiation protocol, and on day 7, Oil Red O staining and Western blotting were performed to confirm adipogenesis. *E*, the relative intensity of the Western blots in *D* was determined in three independent experiments. *F*, C3H10T1/2 cells were transfected with *Ostm1* Stealth™ RNAi at 30% confluence; and after 24 h, they were cultured with a half-dosage of BMP4 (10 ng/ml) until post-confluent and then induced to differentiate with the standard differentiation protocol. *E*, relative intensity of western blotting in *D* was performed through three independent experiments. *, $p < 0.05$; **, $p < 0.01$. *G* and *H*, the accumulation of cytoplasmic triglyceride was detected by Oil Red O staining on day 7, at which point, the cells were photographed. The expression of adipocyte markers (422/aP2 and peroxisome proliferator-activated receptor γ (*PPARγ*)) was also detected with cell extract on day 7. *I*, the relative intensity of the Western blots in *H* was determined in three independent experiments. *I*, relative intensity of western blotting in *H* was performed through three independent experiments. *, $p < 0.05$; **, $p < 0.01$.

includes two sequential processes: lineage commitment into preadipocytes and terminal differentiation into mature adipocytes (3, 4). Compared with the second process, many questions are unresolved concerning commitment. Previously, we showed that C3H10T1/2 cells can commit to adipocyte lineage upon BMP4 treatment (4). In the present study, miR-140, which was previously recognized as a chondrocyte-specific miRNA (25–27, 30–33), was identified as a downstream component of the BMP4 signaling pathway during C3H10T1/2 cell commitment. We consider that it might function as one of the commitment factors. Its overexpression in C3H10T1/2 cells validates our hypothesis. Exogenously expressed miR-140 in C3H10T1/2 cells significantly increases adipocyte differentiation even without BMP4, whereas miR-140 knockdown signif-

icantly decreases adipocyte differentiation. This is the first time that a particular miRNA directly involved in adipocyte lineage commitment has been identified.

Previous studies have shown that miR-140 is prevalently expressed in normal cartilage and regulates cartilage development and homeostasis. The cartilage master regulator SOX9 promotes miR-140 expression. In addition, Postlethwait and co-workers (30) have shown that miR-140 regulates palatogenesis in zebrafish via suppressing PDGF receptor α. Kobayashi and co-workers (33) used miR-140-null mice to demonstrate that miR-140 is essential for normal endochondral bone development and that the miR-140 target *Dnpep* reduces BMP signaling to function in skeletal defects in the mouse model. These results, combined with our research, indicate that miR-140 is essential for mesodermal tissue development and that there is a positive relationship between miR-140 and BMP signaling.

We have identified a direct miR-140 target protein, OSTM1, which is significantly decreased after BMP4 treatment. When we overexpressed *Ostm1* in C3H10T1/2 cells, adipogenic differentiation was significantly decreased, and knockdown led to the opposite result. Therefore, we consider OSTM1 function to be an anti-adipogenic factor in our system. A previous investigation indicates that OSTM1 promotes β-catenin/Lef1 interaction (24). If is well known that the Wnt/β-catenin signaling pathway affects multiple cellular functions, and inhibition of this pathway would favor adipogenesis by mesenchymal stem cells (34, 35). Accordingly, we predict that *Ostm1* repression may lead to a decrease in the Wnt/β-catenin signaling pathway and favor adipogenic differentiation. The crosstalk between the BMP and Wnt pathways has long been recognized and is considered to be an essential growth factor crosstalk that occurs during the entire life of an animal (36). These two signals interact at multiple levels, and our work presents the possibility that OSTM1 may serve as a new linker molecule between the BMP and Wnt pathways.

Nonetheless, a physical process must include combinatorial growth or differentiation signaling repertoires. Other undisclosed miR-140 targets may contribute to adipocyte lineage commitment. Meanwhile, other miRNAs may also function as promotion or suppression factors in adipocyte lineage commitment. More studies are needed to better explain the whole physiological process.

In conclusion, we have demonstrated that miR-140 functions as a positive regulator of adipocyte lineage commitment in response to BMP4 treatment, which in turn decreases *Ostm1* at both the mRNA and protein levels and leads to adipogenesis. This is the first time report that a specific miRNA participates in BMP4-induced C3H10T1/2 adipocyte lineage commitment. Therefore, our results offer new insight into the mechanisms of lineage commitment.

REFERENCES

1. Haslam, D. W., and James, W. P. T. (2005) Obesity. *Lancet* **366,** 1197–1209
2. Kopelman, P. G. (2000) Obesity as a medical problem. *Nature* **404,** 635–643
3. Yu, Z. K., Wright, J. T., and Hausman, G. J. (1997) Preadipocyte recruitment in stromal vascular cultures after depletion of committed preadipocytes by immunocytotoxicity. *Obes. Res.* **5,** 9–15
4. Tang, Q.-Q., Otto, T. C., and Lane, M. D. (2004) Commitment of C3H10T1/2 pluripotent stem cells to the adipocyte lineage. *Proc. Natl. Acad. Sci. U.S.A.* **101,** 9607–9611
5. Tang, Q.-Q., Otto, T. C., and Lane, M. D. (2003) CCAAT/enhancer-binding protein β is required for mitotic clonal expansion during adipogenesis. *Proc. Natl. Acad. Sci. U.S.A.* **100,** 850–855
6. Tang, Q.-Q., and Lane, M. D. (2000) Role of C/EBP homologous protein (CHOP-10) in the programmed activation of CCAAT/enhancer-binding protein-β during adipogenesis. *Proc. Natl. Acad. Sci. U.S.A.* **97,** 12446–12450
7. Rosen, E. D., and MacDougald, O. A. (2006) Adipocyte differentiation from the inside out. *Nat. Rev. Mol. Cell Biol.* **7,** 885–896
8. Zhao, L., Li, G., Chan, K.-M., Wang, Y., and Tang, P.-F. (2009) Comparison of multipotent differentiation potentials of murine primary bone marrow stromal cells and mesenchymal stem cell line C3H10T1/2. *Calcif. Tissue Int.* **84,** 56–64
9. Pinney, D. F., and Emerson, C. P. (1989) 10T1/2 cells: an *in vitro* model for molecular genetic analysis of mesodermal determination and differentiation. *Environ. Health Perspect.* **80,** 221–227
10. Huang, H., Song, T.-J., Li, X., Hu, L., He, Q., Liu, M., Lane, M. D., and Tang, Q.-Q. (2009) BMP signaling pathway is required for commitment of C3H10T1/2 pluripotent stem cells to the adipocyte lineage. *Proc. Natl. Acad. Sci. U.S.A.* **106,** 12670–12675
11. Huang, H.-Y., Hu, L.-L., Song, T.-J., Li, X., He, Q., Sun, X., Li, Y.-M., Lu, H.-J., Yang, P.-Y., and Tang, Q.-Q. (2011) Involvement of cytoskeleton-associated proteins in the commitment of C3H10T1/2 pluripotent stem cells to adipocyte lineage induced by BMP2/4. *Mol. Cell. Proteomics* **10,** M110.002691
12. Bartel, D. P. (2009) MicroRNAs: target recognition and regulatory functions. *Cell* **136,** 215–233
13. Baek, D., Villén, J., Shin, C., Camargo, F. D., Gygi, S. P., and Bartel, D. P. (2008) The impact of microRNAs on protein output. *Nature* **455,** 64–71
14. Alvarez-Garcia, I., and Miska, E. A. (2005) MicroRNA functions in animal development and human disease. *Development* **132,** 4653–4662
15. Gangaraju, V. K., and Lin, H. (2009) MicroRNAs: key regulators of stem cells. *Nat. Rev. Mol. Cell Biol.* **10,** 116–125
16. Alexander, R., Lodish, H., and Sun, L. (2011) MicroRNAs in adipogenesis and as therapeutic targets for obesity. *Expert Opin. Ther. Targets* **15,** 623–636
17. Yi, C., Xie, W., Li, F., Lv, Q., He, J., Wu, J., Gu, D., Xu, N., and Zhang, Y. (2011) MiR-143 enhances adipogenic differentiation of 3T3-L1 cells through targeting the coding region of mouse pleiotrophin. *FEBS Lett.* **585,** 3303–3309
18. Wang, Q., Li, Y. C., Wang, J., Kong, J., Qi, Y., Quigg, R. J., and Li, X. (2008) miR-17-92 cluster accelerates adipocyte differentiation by negatively regulating tumor-suppressor Rb2/p130. *Proc. Natl. Acad. Sci. U.S.A.* **105,** 2889–2894
19. Ling, H.-Y., Wen, G.-B., Feng, S.-D., Tuo, Q.-H., Ou, H.-S., Yao, C. H., Zhu, B.-Y., Gao, Z.-P., Zhang, L., and Liao, D.-F. (2011) MicroRNA-375 promotes 3T3-L1 adipocyte differentiation through modulation of extracellular signal-regulated kinase signalling. *Clin. Exp. Pharmacol. Physiol.* **38,** 239–246
20. Kim, S. Y., Kim, A. Y., Lee, H. W., Son, Y. H., Lee, G. Y., Lee, J.-W., Lee, Y. S., and Kim, J. B. (2010) miR-27a is a negative regulator of adipocyte differentiation via suppressing PPARγ expression. *Biochem. Biophys. Res. Commun.* **392,** 323–328
21. Jennewein, C., von Knethen, A., Schmid, T., and Brüne, B. (2010) MicroRNA-27b contributes to lipopolysaccharide-mediated peroxisome proliferator-activated receptor γ (PPARγ) mRNA destabilization. *J. Biol. Chem.* **285,** 11846–11853
22. Leisle, L., Ludwig, C. F., Wagner, F. A., Jentsch, T. J., and Stauber, T. (2011) ClC-7 is a slowly voltage-gated $2Cl^-/1H^+$-exchanger and requires Ostm1 for transport activity. *EMBO J.* **30,** 2140–2152
23. Fischer, T., De Vries, L., Meerloo, T., and Farquhar, M. G. (2003) Promotion of $G\alpha_{i3}$ subunit down-regulation by GIPN, a putative E3 ubiquitin ligase that interacts with RGS-GAIP. *Proc. Natl. Acad. Sci. U.S.A.* **100,** 8270–8275
24. Feigin, M. E., and Malbon, C. C. (2008) OSTM1 regulates β-catenin/Lef1

interaction and is required for Wnt/β-catenin signaling. *Cell. Signal.* **20,** 949–957
25. Tuddenham, L., Wheeler, G., Ntounia-Fousara, S., Waters, J., Hajihosseini, M. K., Clark, I., and Dalmay, T. (2006) The cartilage-specific microRNA-140 targets histone deacetylase 4 in mouse cells. *FEBS Lett.* **580,** 4214–4217
26. Nakamura, Y., He, X., Kobayashi, T., Yan, Y.-L., Postlethwait, J. H., and Warman, M. L. (2008) Unique roles of microRNA-140 and its host gene *WWP2* in cartilage biology. *J Musculoskelet. Neuronal Interact.* **8,** 321–322
27. Yang, J., Qin, S., Yi, C., Ma, G., Zhu, H., Zhou, W., Xiong, Y., Zhu, X., Wang, Y., He, L., and Guo, X. (2011) MiR-140 is co-expressed with *Wwp2-C* transcript and activated by Sox9 to target *Sp1* in maintaining the chondrocyte proliferation. *FEBS Lett.* **585,** 2992–2997
28. Thomas, M., Lieberman, J., and Lal, A. (2010) Desperately seeking microRNA targets. *Nat. Struct. Mol. Biol.* **17,** 1169–1174
29. Gesta, S., Tseng, Y.-H., and Kahn, C. R. (2007) Developmental origin of fat: tracking obesity to its source. (2007) *Cell* **131,** 242–256
30. Eberhart, J. K., He, X., Swartz, M. E., Yan, Y.-L., Song, H., Boling, T. C., Kunerth, A. K., Walker, M. B., Kimmel, C. B., and Postlethwait, J. H. (2008) MicroRNA Mirn140 modulates Pdgf signaling during palatogenesis. *Nat. Genet.* **40,** 290–298
31. Miyaki, S., Sato, T., Inoue, A., Otsuki, S., Ito, Y., Yokoyama, S., Kato, Y., Takemoto, F., Nakasa, T., Yamashita, S., Takada, S., Lotz, M. K., Ueno-Kudo, H., and Asahara, H. (2010) MicroRNA-140 plays dual roles in both cartilage development and homeostasis. *Genes Dev.* **24,** 1173–1185
32. Araldi, E., and Schipani, E. (2010) MicroRNA-140 and the silencing of osteoarthritis. *Genes Dev.* **24,** 1075–1080
33. Nakamura, Y., Inloes, J. B., Katagiri, T., and Kobayashi, T. (2011) Chondrocyte-specific microRNA-140 regulates endochondral bone development and targets *Dnpep* to modulate bone morphogenetic protein signaling. *Mol. Cell. Biol.* **31,** 3019–3028
34. Cho, S. W., Yang, J.-Y., Sun, H. J., Jung, J. Y., Her, S. J., Cho, H. Y, Choi, H. J., Kim, S. W., Kim, S. Y., and Shin, C. S. (2009) Wnt inhibitory factor (WIF)-1 inhibits osteoblastic differentiation in mouse embryonic mesenchymal cells. *Bone* **44,** 1069–1077
35. Bilkovski, R., Schulte, D. M., Oberhauser, F., Gomolka, M., Udelhoven, M., Hettich, M. M., Roth, B., Heidenreich, A., Gutschow, C., Krone, W., and Laudes, M. (2010) Role of Wnt-5a in the determination of human mesenchymal stem cells into preadipocytes. *J. Biol. Chem.* **285,** 6170–6178
36. Winkler, D. G., Sutherland, M. S., Ojala, E., Turcott, E., Geoghegan, J. C., Shpektor, D., Skonier, J. E., Yu, C., and Latham, J. A. (2005) Sclerostin inhibition of Wnt-3a-induced C3H10T1/2 cell differentiation is indirect and mediated by bone morphogenetic proteins. *J. Biol. Chem.* **280,** 2498–2502